Geoscience Frontiers 12 (2021) 1031–1037

HOSTED BY

Contents lists available at ScienceDirect

Geoscience Frontiers

journal homepage: www.elsevier.com/locate/gsf

Research Paper

High-pressure investigations on the isostructural phase transition and metallization in realgar with diamond anvil cells

Linfei Yang [a,b], Lidong Dai [a,*], Heping Li [a], Haiying Hu [a], Meiling Hong [a,b], Xinyu Zhang [a,b], Pengfei Liu [c]

[a] Key Laboratory of High-Temperature and High-Pressure Study of the Earth's Interior, Institute of Geochemistry, Chinese Academy of Sciences, Guiyang, Guizhou, 550081, China
[b] University of Chinese Academy of Sciences, Beijing, 100049, China
[c] State Key Laboratory of Structural Chemistry, Fujian Institute of Research on the Structure of Matter, Chinese Academy of Sciences, Fuzhou, Fujian, 350002, China

ARTICLE INFO

Keywords:
Realgar
Isostructural phase transition
Metallization
Raman spectroscopy
Electrical conductivity
High pressure

ABSTRACT

The high-pressure structural, vibrational and electrical properties for realgar were investigated by in-situ Raman scattering and electrical conductivity experiments combined with first-principle calculations up to ~30.8 GPa. It was verified that realgar underwent an isostructural phase transition at ~6.3 GPa and a metallization at a higher pressure of ~23.5 GPa. The isostructural phase transition was well evidenced by the obvious variations of Raman peaks, electrical conductivity, crystal parameters and the As–S bond length. The phase transition of metallization was in closely associated with the closure of bandgap rather than caused by the structural phase transition. And furthermore, the metallic realgar exhibited a relatively low compressibility with the unit cell volume V_0 = 718.1.4 Å^3 and bulk modulus B_0 = 36.1 GPa.

1. Introduction

Arsenic sulfides have attracted lots of scientific interests because of their wide industrial applications and unique physical properties, such as strong infrared transparency, high sensitivity to light radiation and outstanding ability of doping (Kyono et al., 2005; Bonazzi et al., 2006; Naumov et al., 2007; Hejny et al., 2012). Within the system of As–S, there exist two fundamental arsenic sulfide minerals including realgar (As_4S_4) and orpiment (As_2S_3), and moreover, other intermediate compounds with the chemical composition of $As_{1-x}S_x$ have also been widely reported (Lowe et al. 2006; Bonazzi and Bindi, 2008). Realgar is a representative arsenic sulfide mineral, which is usually found in the epithermal deposits and volcanic fumaroles. In some Carlin-type gold deposits, the realgar often occurs together with gold-bearing ores, and the ore-forming elements including As, S and Au were deemed to mainly originate from the mantle (Zhang et al., 2010; Wang et al., 2012). As an important source of elemental arsenic and sulfur, it is possible that the realgar will enter into the deep mantle and accompany to release these ore-forming materials in geological process. In fact, many recent studies have clearly shown that there are at least a part of sulfides subducting to the deep mantle (Hattori et al., 2002; Jego and Dasgupta, 2013; Evans et al., 2014). And thus, the investigation on the structural stability of realgar under high pressure is crucial to understand the sulfur and arsenic recycling in the interior of Earth.

At ambient conditions, realgar exhibits a semiconducting characteristic with the bandgap energy of 2.00 eV. It crystallizes into a monoclinic and cage-like molecular structure with the space group of $P2_1/n$: there are four separate As_4S_4 molecules in the unit cell, which are mutually linked by the weak van der Waals forces; in each As_4S_4 molecule, one As atom is directly connected to another one As atom and two S atoms by the covalent bond. This unique cage-like molecular structure in realgar provokes great interests to investigate its structural stability under conditions of exposure to light, high temperature and high pressure. Naumov et al. (2007) studied the effect of light radiation on the crystal structure of realgar using the single-crystal X-ray photodiffraction and Fourier transform infrared spectroscopy, and a photo-induced phase transition from realgar to pararrealgar was observed. Hall (1966) reported that realgar transformed to a new phase of β-As_4S_4 (space group: C_2/c) at a high temperature of ~529 K and under room pressure. As for the influence of pressure on the structural properties of realgar, there exist some

* Corresponding author.
E-mail address: dailidong@vip.gyig.ac.cn (L. Dai).
Peer-review under responsibility of China University of Geosciences (Beijing).

https://doi.org/10.1016/j.gsf.2020.05.017
Received 5 December 2019; Received in revised form 11 March 2020; Accepted 20 May 2020
Available online 21 June 2020

controversial viewpoints among previously reported results. Tuktabiev et al. (2009) carried out high-pressure energy-dispersive X-ray diffraction measurements for realgar up to ~8.0 GPa to explore its structural variations with pressure, and a ~7.0 GPa of structural phase transition was verified by the abrupt collapse of unit cell volume. In contrast, Hejny et al. (2012) did not observe this phase transition and found that realgar remained stable monoclinic structure up to ~17.4 GPa, which was evidenced by the results of X-ray diffraction, optical absorption and vibration spectroscopy measurements. And therefore, more systematical investigations on the high-pressure structural behavior of realgar are urgently needed.

In addition, a recent work by Liu et al. (2019) revealed that orpiment underwent a pressure-induced electronic phase transition from semiconductor to metal at ~42.0 GPa. As a similar arsenic sulfide, realgar might also exhibit metallic characteristics under high pressure. As we know, the metallization transition can be efficiently detected by high-pressure electrical conductivity measurements (Zhao et al., 2015; Wang et al., 2017; Naumov et al. 2018). However, to the best of our knowledge, relative experimental investigations on the electrical property of realgar under high pressure are still blank till now.

In this study, we carried out a series of Raman scattering and electrical conductivity experiments along with the first-principle calculations in a diamond anvil cell under high pressure up to ~30.8 GPa, mainly aiming to understand the crystal and electronic structure variations of realgar under high pressure. Two pressure-induced phase transitions for realgar have been well determined and discussed in detail.

2. Experimental methods

The natural crystalline realgar was obtained from Longtang diggings in Nanhua County, Yunnan Province. It was ground into micron-sized powders by the agate mortar, and then the powder realgar was used as the starting sample for all of high-pressure experiments. The symmetric diamond anvil cell (DAC) with anvil culet face of 300 μm was employed to generate high pressure environments. A small ruby chip was loaded into the center of sample chamber to calibrate the pressure based on the shifts of R_1 fluorescence lines (Mao et al., 1986). Raman spectra were collected in the wavenumber range of 100–600 cm^{-1} using a micro-confocal Invia Raman spectrometer (Renishaw, England) along with a 514.5 nm of argon ion laser. The laser power and collection time for each collected Raman spectra were set to 20 mW and 120 s, respectively. The electrical conductivity measurements were carried out with a Solartron-1260 impedance/gain phase analyzer (Solartron, the United Kingdom), and the impedance spectra were acquired in the frequency range of 10^{-1}–10^{7} Hz. Using the laser drilling device, a 100 μm of hole was drilled in the T-301 stainless steel as the sample chamber. This hole was surrounded by the compressed insulating materials, which are composed of the mixture of boron nitride and epoxy powders. No pressure medium materials were used in our electrical conductivity experiments to avoid the influence of external impurities. The first-principle calculations were conducted using the CASTEP code in the Material Studio software to predict the structural and electrical behavior of realgar under high pressure. The generalized gradient approximation (GGA) was used as the exchange-correlation functional. To ensure the full convergence of the total energy calculation, we chose a 450 eV of cutoff energy and a 6 × 6 × 6 of K-point grid. More detailed information on the experimental procedures and theoretical calculation methods has been illustrated in previous work (Dai et al., 2017, 2018; 2019; Liu et al., 2017; Zhuang et al., 2017; Yang et al., 2019).

3. Results and discussion

3.1. Phase transitions in realgar under high pressure

The vibrational properties of realgar were explored by Raman spectroscopic measurements under high pressure up to ~30.8 GPa and room temperature. Fig. 1 displays the collected Raman spectra of realgar at ambient conditions. In order to make precise fits and obtain Raman peak values from the data, we select the Gauss function to fit the Raman spectra as shown in the inset diagram. Ten Raman-active peaks have been acquired in this study, i.e., 182 cm^{-1}, 195 cm^{-1}, 220 cm^{-1}, 231 cm^{-1}, 268 cm^{-1}, 307 cm^{-1}, 323 cm^{-1}, 340 cm^{-1}, 358 cm^{-1} and 364 cm^{-1}. The most intense peak at 340 cm^{-1} stands for the As–S antisymmetric stretching mode, and the peaks at 182 cm^{-1}, 195 cm^{-1} and 220 cm^{-1} are assigned to the A_1, B_1 and E deformation modes, respectively (Forneris, 1969). All of the observed Raman peaks for realgar are in good agreement with previous reported data by Cheng et al. (2017). Fig. 2a shows the Raman spectra of realgar in the pressure range from ~0.8 GPa to ~30.8 GPa and under room temperature, and the corresponding pressure dependence of Raman shifts for all of the vibrational modes are presented in Fig. 2b. Two discontinuous points can be clearly observed at pressures of ~6.3 GPa and ~23.5 GPa, respectively. At ~6.3 GPa, Raman peaks at 231 cm^{-1} and 340 cm^{-1} both exhibit obvious variations in their pressure dependence and suddenly become weakening and broadening. At the same time, other peaks disappear. When the pressure further increases to ~23.5 GPa, the peaks at 231 cm^{-1} and 340 cm^{-1} display relatively weak pressure dependences. It is well known that the high-pressure Raman spectroscopy is a very efficient method to detect structural or electronic changes of minerals. And thus, the variations in the pressure dependence of Raman shifts observed in this study imply that realgar might undergo two pressure-induced phase transitions at ~6.3 GPa and ~23.5 GPa, respectively.

In order to check the pressure-induced phase transitions in realgar, we carried out electrical conductivity measurements under high pressure and room temperature. Typical impedance spectra for realgar under high pressure up to ~30.3 GPa are shown in Fig. 3a–c. In the pressure range of 0.8–21.3 GPa, each impedance spectra exhibits two obvious semicircular arcs and locates in the first quadrant, which represents grain interior and boundary resistance, respectively. However, at higher pressure range of 23.5–30.3 GPa, only the grain interior arc appears in the fourth quadrant and the grain boundary contribution disappears. This abrupt variation indicates that the electronic structure of realgar has been greatly changed above ~23.5 GPa, and it can be attributed to the pressure-induced electronic polarization (Kandrina et al., 2002). Fig. 3d displays the pressure-dependent electrical conductivity of realgar in the whole

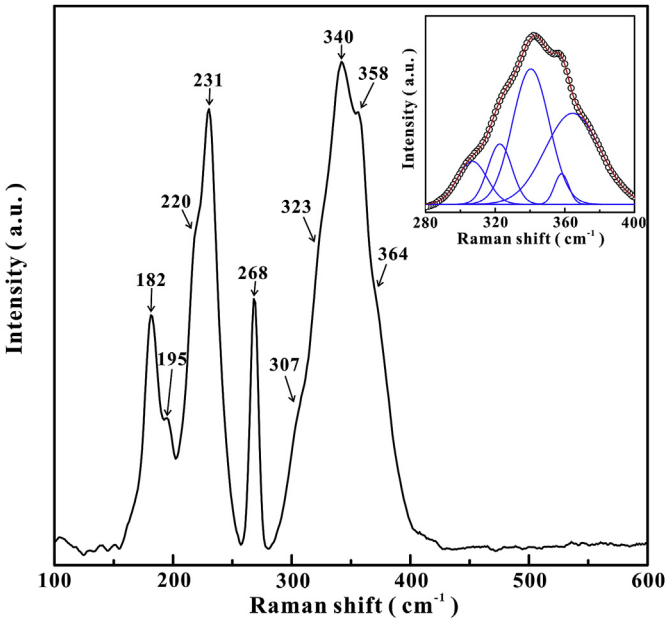

Fig. 1. Raman spectra of realgar in the frequency range from 100 cm^{-1} to 600 cm^{-1} under room temperature and pressure. Insert: the representative fitting result of Raman spectra by the Gauss function.

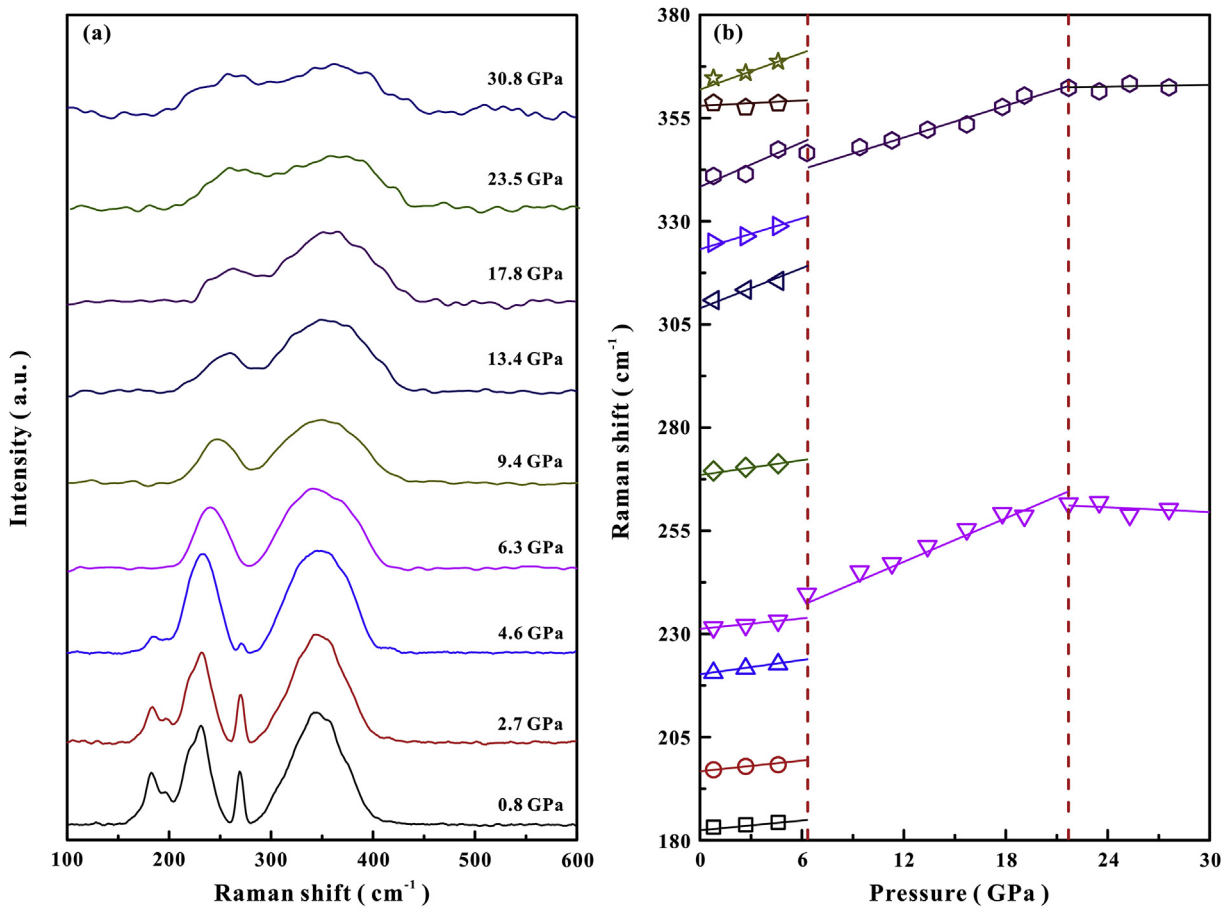

Fig. 2. (a) Raman spectra for realgar in the pressure range of 0.8–30.8 GPa. (b) The corresponding pressure dependence of Raman shifts for all of the obtained modes.

pressure range, which was obtained by fitting the impedance spectra using the equivalent circuit method (Dai et al., 2016; Hu et al., 2018). Three distinct regions can be clearly observed on the basis of the slope variation of electrical conductivity upon compression as follows: (i) at 0.8–6.5 GPa, the electrical conductivity of realgar gradually decreases with increasing pressure, and the corresponding slope is determined to be -0.08 S cm^{-1} GPa^{-1}; (ii) at 6.5–23.5 GPa, it shows a positive pressure dependence with a slope of ~0.07 S cm^{-1} GPa^{-1}; (iii) at 23.5–30.3 GPa, the electrical conductivity tends to be stable and displays a relatively high value of 2.8 S cm^{-1}. When the pressure is released, the electrical conductivity of realgar still remains very high values instead of recovering to its original magnitude.

As for the first slope variation of electrical conductivity for realgar at ~6.5 GPa, it implies that realgar undergoes a pressure-induced structural phase transition at this pressure point. In fact, in terms of the issue of the phase stability of realgar under high pressure, previously reported results are inconsistent. Tuktabiev et al. (2009) carried out the energy-dispersive X-ray diffraction measurements to investigate the structural evolution of realgar under high pressure to ~8.0 GPa, and found that realgar endured a structural phase transition at ~7.0 GPa. In contrast, Hejny et al. (2012) did not observe any phase transition in realgar from the in-situ X-ray diffraction experiments up to ~17.4 GPa. In this study, our electrical conductivity results provide favorable evidences for the phase transition of realgar occurring at ~6.5 GPa. This result is simialr to that reported by Tuktabiev et al. (2009) although the transition point is slightly lower than their data. The discrepacy is possibly caused by the different measurement method and the magnitude of deviatoric stress in the sample chamber. It is well known that the deviatoric stress can significantly influence the high-pressure physical properties of some minerals and materials (Dai et al., 2017, 2018, 2019). However, our results are different from the work by Hejny et al. (2012), who failed to detect any phase transitions in natural realgar. It should be mentioned that the composition of their starting realgar contained some impurities of Sn (~0.23 wt.%) and Sb (~0.86 wt.%), which might result in these discrepcaies. In light of the second pressure inflection point of ~23.5 GPa above which the electrical conductivity exhibits weak pressure dependence, it provides an important clue to characterize a pressure-induced electronic phase transition for realgar from semiconductor to metal at ~23.5 GPa. As we know, the increase rate of carrier concentration with pressure would be significantly decreased once the pressure-induced metallization occurs, which leads to the weak pressure dependence of electrical conductivity. In fact, the phenomenon of weak pressure dependence has also been observed in other metallized materials, such as $MoSe_2$, Sb_2S_3 and VO_2 (Bai et al., 2015; Dai et al., 2018; Yang et al., 2019). In particular, the unrecoverable electrical conductivity of realgar during decompression indicates that the metallization is irreversible. In addition, other similar sulfides, such as Sb_2S_3, MoS_2, ReS_2, have also been found to undergo metallization under high pressure, indicating that the metallization phase transition might be a common phenomenon for most of sulfides (Hromadová et al., 2013; Chi et al., 2014; Nayak et al., 2014; Dai et al., 2018; Wang et al., 2018).

To further reveal the type of the structural phase transition and explore the metallization mechanism for realgar, the first-principle calculations were carried out up to ~30 GPa. As shown in Fig. 4a, it can be seen that the bandgap energy at ambient conditions is ~2.00 eV, which is 17% lower than the previously reported value of ~2.40 eV by Street and Gill (1966) and 13% lower than the value of 2.30 eV obtained from Skettrup (1978). These slight discrepancies are due to that the density functional theory (DFT) calculation employed in this study usually underestimates the bandgap energy (Errandonea et al., 2005). With

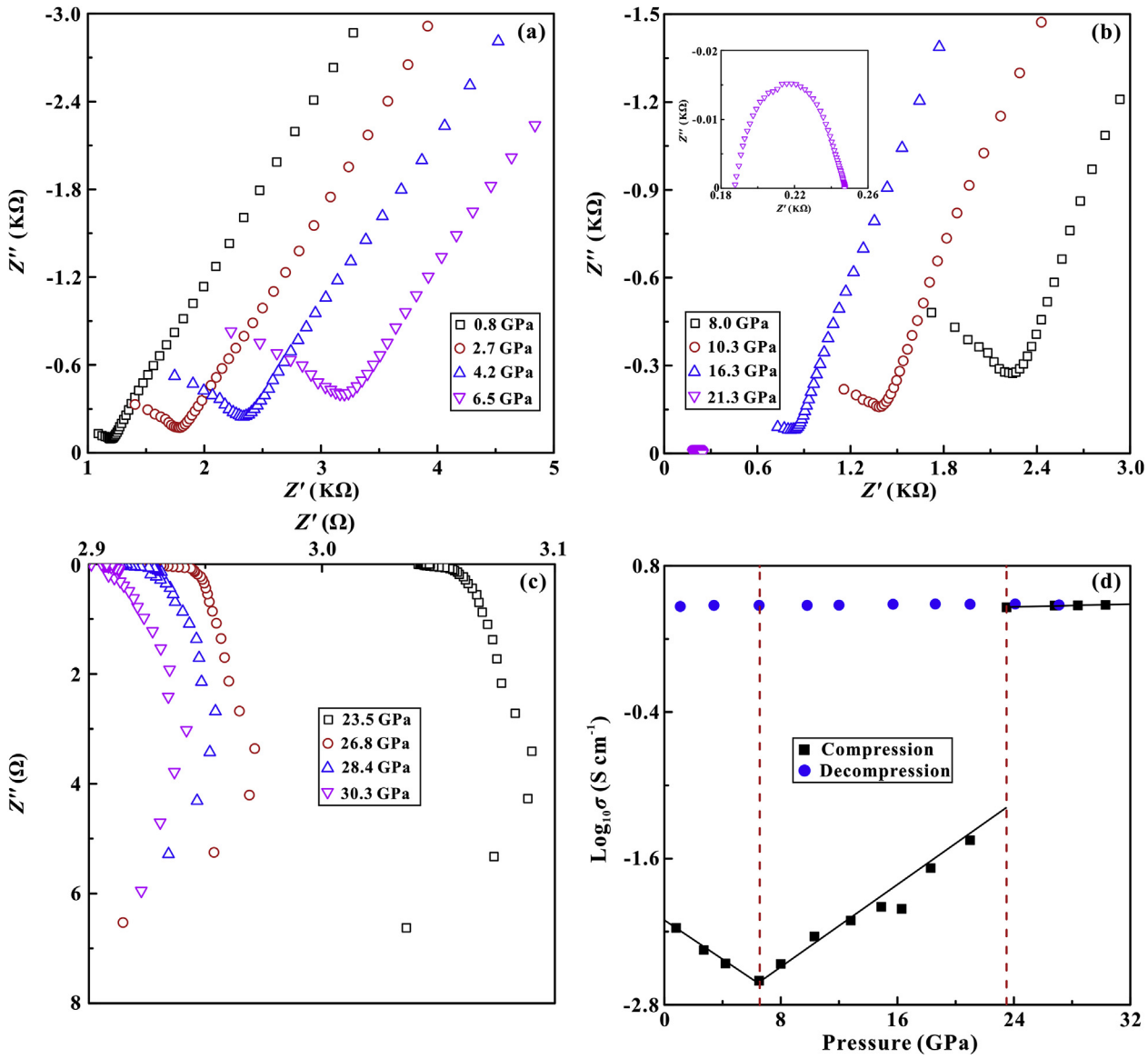

Fig. 3. (a–c) Representative impedance spectra of realgar at pressures of 0.8–30.3 GPa. (d) The pressure-dependent electrical conductivity of realgar upon compression and decompression.

increasing pressure from 0 GPa to 22 GPa, the bandgap energy of realgar shows a gradually decreasing tendency. When the pressure is enhanced to ~24 GPa, the bandgap energy decreases to a critical value of 0 eV, implying that the realgar transforms to a metallic phase. In addition, as plotted in Fig. 4b–e, we also present the band structure, total and partial density of state at selected pressures of 0 GPa and 24 GPa to disclose the electronic structural characteristic before and after metallization of realgar. At 0 GPa, the top of the valence bands (VB) is mainly composed of the S-*p* electronic orbits, and the bottom of the conduction bands (CB) is dominated by the As-*p* electronic orbits. At 24 GPa, all of the electronic orbits become greatly expanded and the conduction bands across the Fermi-level (E_F) to slightly overlap with the valence bands (VB). This predicted metallization pressure point is in good agreement with the results obtained from Raman and electrical conductivity experiments.

At the same time, as shown in Fig. 5, some crucial physical parameters including the ratio of crystal parameter, unit cell volume and bond length have been calculated to predict the structural evolution of realgar under high pressure. From Fig. 5a, it can be clearly seen that the compressibility of realgar is strongly anisotropic: the crystal axis of *b* has the largest compressibility, while the *a* axis exhibits the weakest compression behavior. One previous work by Hejny et al. (2012) also revealed that the compressibility of *b* axis in realgar was the largest. More specifically, the calculated lattice constant ratios of a/a_0, b/b_0 and c/c_0 exhibit continuous variations with pressure up to 30 GPa, implying the absence of the first-order phase transition for realgar in the given pressure range. However, the *a*/*c*, *a*/*b* and the intermolecular distance of S1–As2, S2–As3 and S3–As4 display an obvious discontinuous variation at 6 GPa as presented in Fig. 5b and c. It provides an important evidence to indicate that realgar undergoes an isostructural phase transition at 6 GPa. Fig. 5d reflects the pressure-dependent unit cell volume of realgar. Obviously, the unit cell volume gradually decreases with pressure and no volume collapse can be observed, which further verifies the absence of the first-order phase transition in realgar under high pressure up to 30 GPa. And furthermore, the *P*–*V* data of unit cell volume obtained from our theoretical calculations are fitted by the common third-order Birch–Murnaghan equation of state as follows:

$$P=\frac{3B_0}{2}\left[\left(\frac{V_0}{V}\right)^{\frac{7}{3}}-\left(\frac{V_0}{V}\right)^{\frac{5}{3}}\right]\left\{1+\frac{3}{4}\left(B_0^{'}-4\right)\left[\left(\frac{V_0}{V}\right)^{\frac{2}{3}}-1\right]\right\} \quad (1)$$

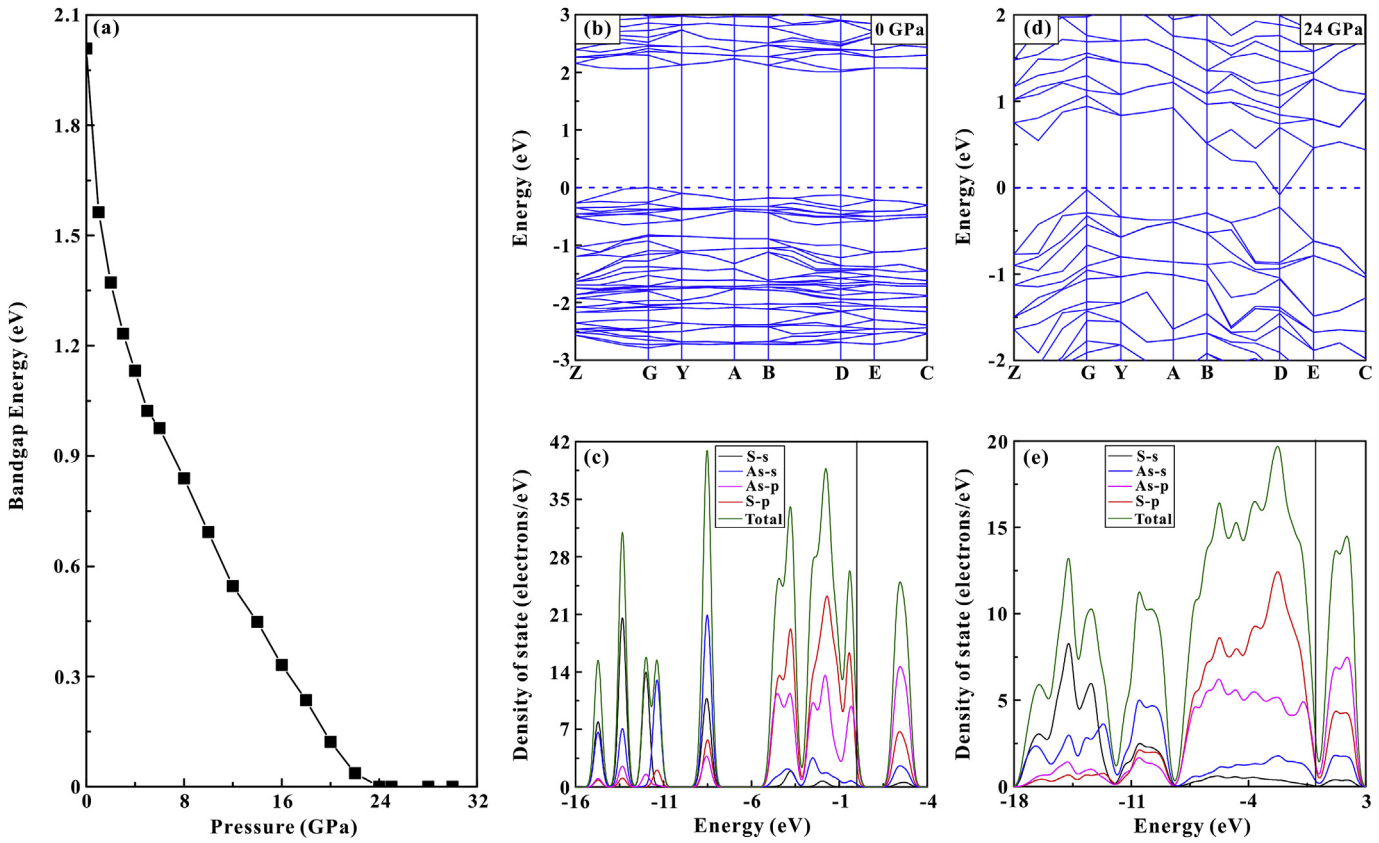

Fig. 4. (a) The bandgap energy of realgar with increasing pressure up to 30 GPa. (b) and (d) The band structure of realgar at 0 GPa and 24 GPa, respectively. (c) and (e) The total and partial density of state for realgar at 0 GPa and 24 GPa, respectively.

where B_0, B_0' and V_0 represent the bulk modulus, first-order derivative of the bulk modulus and unit cell volume at zero pressure, respectively. The first-order derivative of the bulk modulus (B_0') is fixed to 4 at different pressure ranges. At 0–6 GPa, the fitting results for the semiconducting realgar yield $B_0 = 11.4$ GPa and $V_0 = 864.4$ Å^3, which is in consistent with the data reported by Hejny et al. (2012). At 6–24 GPa, the B_0 and V_0 for the isostructural new phase are determined to be 28.3 GPa and 752.0 Å^3. At 24–30 GPa, the corresponding fitting results for the metallic phase yield $B_0 = 36.1$ GPa and $V_0 = 718.1.4$ Å^3. In comparison with the semiconducting realgar and the isostructural new phase, a relatively high value of bulk modulus in the metallic realgar indicates the low crystal compressibility above 24 GPa.

And therefore, it can be concluded that our results from Raman spectroscopy, electrical conductivity and first-principle calculations provide consistent evidences to support two pressure-induced phase transitions in realgar at ~6 GPa and ~24 GPa, respectively. Furthermore, the results obtained by the first-principle calculations reveal that the transformation at ~6 GPa is related to a pressure-induced isostructural phase transition, and the new phase still remains monoclinic structure. The transition at a higher pressure of ~24 GPa is attributed to an electronic phase transition from semiconductor to metal. As for the metallization mechanism of realgar occurring at ~24 GPa, we think that it is just a result of the gradual closure of bandgap rather than triggered by the structural phase transition. In addition, some crucial comparisons between realgar (As_4S_4) and orpiment (As_2S_3) have been conducted in this study. As a similar layered sulfide, orpiment has also been reported to undergo a pressure-induced isostructural phase transition followed by the occurrence of metallization (Liu et al., 2019). However, in comparison with orpiment, the transformation pressure points for isostructural phase transition and metallization in realgar are much lower by nearly 19 GPa and 24 GPa, respectively. This strongly indicates that the crystal and electronic structure of realgar is much more sensitive to pressure than orpiment.

3.2. Implications for the arsenic recycling in the interior of earth

The arsenic content in the mantle is a basic and important geological issue. Many previous studies have provided evidences for the enrichment of arsenic in the mantle, and the subducting slabs containing the arsenic-bearing minerals were considered to release the arsenic element into mantle wedges (Bulanova et al., 1996; Noll et al., 1996; Hattori et al., 2002). As a typical arsenic-bearing mineral for realgar, the investigation on its structural, vibrational and electrical properties under high pressure can provide a deep insight into the arsenic recycling in the interior of Earth. Our results clearly revealed that the monoclinic structure of realgar could remain stable up to ~30 GPa, but its electrical conductivity was greatly increased by about three orders of magnitude after the pressure-induced metallization phase transition. This indicates that realgar has the potential to enter into the deep mantle in the subduction zone as the source of arsenic. More importantly, its exhibited high electrical conductivity under high pressure might influence the electrical property of mantle.

4. Conclusions

In summary, we carried out a series experimental measurements and theoretical calculations to systematically study the effect of pressure on the crystal structural evolution, optical and electrical behavior of realgar. Raman scattering results clearly reveal that there exist two phase transitions in realgar occurring at ~6.3 GPa and ~23.5 GPa, respectively. The

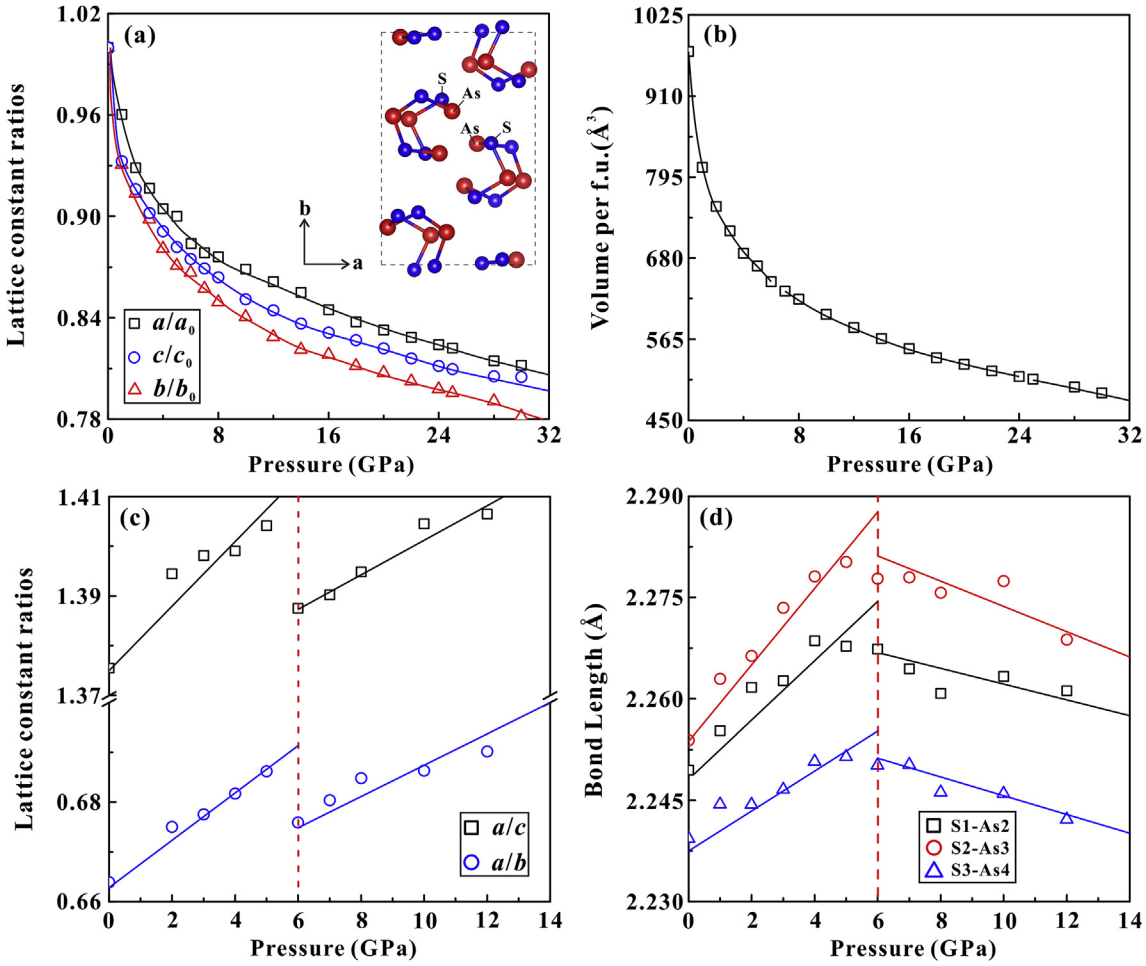

Fig. 5. (a) The calculated lattice parameters of realgar as a function of pressure, including a/a_0, b/b_0 and c/c_0. The insert image: the crystal structure of realgar in the view of *ab* plane at ambient conditions. (b) The unit cell volume of realgar with increasing pressure. (c) The lattice constant ratios for a/c and a/b with pressure. (d) The pressure dependence of bond length for S1–As2, S2–As3 and S3–As4.

results from electrical conductivity measurements exhibit two inflection pressure points at ~6.5 GPa and ~23.5 GPa, which implies that realgar undergoes a pressure-induced isostructural phase transition and an electronic transformation from semiconductor to metal. The first-principle calculations further revealed the nature of the metallization in realgar: it is not triggered by a structural phase transition, but strongly related with the gradual closure of bandgap.

Declaration of competing interest

The authors declare that they have no known competing financial interests or personal relationships that could have appeared to influence the work reported in this paper.

Acknowledgements

This research was financially supported by the strategic priority Research Program (B) of the Chinese Academy of Sciences (Grant No. 18010401), Key Research Program of Frontier Sciences of CAS (Grant No. QYZDB-SSW-DQC009), Hundred Talents Program of CAS, NSF of China (Grant Nos. 41774099 and 41772042), Youth Innovation Promotion Association of CAS (Grant No. 2019390) and Special Fund of the West Light Foundation of CAS. The support of the Supercomputer Center of Fujian Institute of Research on the Structure of Matter (FJIRSM) is acknowledged.

References

Bai, L., Li, Q., Corr, S.A., Meng, Y., Park, C., Sinogeikin, S.V., K.,C., Wu, J., Shen, G., 2015. Pressure-induced phase transitions and metallization in VO_2. Phys. Rev. B 91, 104110.

Bonazzi, P., Bindi, L., Pratesi, G., Menchetti, S., 2006. Light-induced changes in molecular arsenic sulfides: state of the art and new evidence by single-crystal X-ray diffraction. Am. Mineral. 91, 1323–1330.

Bonazzi, P., Bindi, L., 2008. A crystallographic review of arsenic sulfides: effects of chemical variations and changes induced by exposure to light. Z. Kristallogr. 223, 132–147.

Bulanova, G.P., Griffin, W.L., Ryan, C.G., Shestakova, O.Y., Barnes, S.J., 1996. Trace elements in sulfide inclusions from Yakutian diamonds. Contrib. Mineral. Petrol. 124, 111–125.

Cheng, H., Zhou, Y., Frost, R.L., 2017. Structure comparison of orpiment and realgar by Raman spectroscopy. Spectrosc. Lett. 50, 23–29.

Chi, Z.H., Zhao, X.M., Zhang, H., Goncharov, A.F., Lobanov, S.S., Kagayama, T., Sakata, M., Chen, X.J., 2014. Pressure-induced metallization of molybdenum disulfide. Phys. Rev. Lett. 113, 036802.

Dai, L., Hu, H., Li, H., Wu, L., Hui, K., Jiang, J., Sun, W., 2016. Influence of temperature, pressure, and oxygen fugacity on the electrical conductivity of dry eclogite, and geophysical implications. G-cubed 17, 239–2407.

Dai, L., Zhuang, Y., Li, H., Wu, L., Hu, H., Liu, K., Yang, L., Pu, C., 2017. Pressure-induced irreversible amorphization and metallization with a structural phase transition in arsenic telluride. J. Mater. Chem. C 5, 12157–12162.

Dai, L., Liu, K., Li, H., Wu, L., Hu, H., Zhuang, Y., Yang, L., Pu, C., Liu, P., 2018. Pressure-induced irreversible metallization accompanying the phase transitions in Sb_2S_3. Phys. Rev. B 97, 024103.

Dai, L., Pu, C., Li, H., Hu, H., Liu, K., Yang, L., Hong, M., 2019. Characterization of metallization and amorphization for GaP under different hydrostatic enviroments in diamond anvil cell up to 40.0 GPa. Rev. Sci. Instrum. 90, 066103.

Errandonea, D., Segura, A., Manjón, F.J., Chevy, A., Machado, E., Tobias, G., Ordejón, P., Canadell, E., 2005. Crystal symmetry and pressure effects on the valence band structure of γ-InSe and ε-GaSe: transport measurements and electronic structure calculations. Phys. Rev. B 71, 125206.

Evans, K.A., Tomlins, A.G., Cliff, J., Fiorentini, M.L., 2014. Insights into subduction zone sulfur recycling from isotopic analysis of eclogite-hosted sulfides. Chem. Geol. 365, 1–19.

Forneris, R., 1969. The infrared and Raman spectra of realgar and orpiment. Am. Mineral. 54, 1062–1074.

Hall, H.T., 1966. The System Ag-Sb-S, Ag-As-S, and Ag-Bi-S: Phase Relations and Mineralogical Significance. Ph.D thesis. Brown University.

Hattori, K.H., Arai, S., Clarke, D.B., 2002. Selenium, tellurium, arsenic and antimony contents of primary mantle sulfides. Can. Mineral. 40, 637–650.

Hejny, C., Sagl, R., Többens, D.M., Miletich, R., Wildner, M., Nasdala, L., Ullrich, A., Balic-Zunic, T., 2012. Crystal-structure properties and the molecular nature of hydrostatically compressed realgar. Phys. Chem. Miner. 39, 399–412.

Hromadová, L., Martoňák, R., Tosatti, E., 2013. Structure change, layer sliding, and metallization in high-pressure MoS_2. Phys. Rev. B 87, 144105.

Hu, H., Dai, L., Li, H., Sun, W., Li, B., 2018. Effect of dehydrogenation on the electrical conductivity of Fe-bearing amphibole: implications for high conductivity anomalies in subduction zones and continental crust. Earth Planet Sci. Lett. 498, 27–37.

Jego, S., Dasgupta, R., 2013. Fluid-present melting of sulfide-bearing ocean-crust: experimental constraints on the transport of sulfur from subducting slab to mantle wedge. Geochem. Cosmochim. Acta 110, 106–134.

Kandrina, Y.A., Babushkin, A.N., Shkerin, S.N., Volkova, Y.Y., 2002. Application of the AC impedance spectroscopy at high pressures: electrophysical properties of sulfur. Defect Diffusion Forum 208–209, 295–298.

Kyono, A., Kimata, M., Hatta, T., 2005. Light-induced degradation dynamics in realgar: in situ structural investigation using single-crystal X-ray diffraction study and X-ray photoelectron spectroscopy. Am. Mineral. 90, 1563–1570.

Liu, K., Dai, L., Li, H., Hu, H., Wu, L., Zhuang, Y., Pu, C., Yang, L., 2017. Migration of impurity level reflected in the electrical conductivity variation for natural pyrite at high temperature and high pressure. Phys. Chem. Miner. 45, 85–92.

Liu, K., Dai, L., Li, H., Hu, H., Yang, L., Pu, C., Hong, M., Liu, P., 2019. Phase transition and metallization of orpiment by Raman spectroscopy, electrical conductivity and theoretical calculation under high pressure. Materials 12, 784.

Lowe, A.J., Elliott, S.R., Greaves, G.N., 2006. Extended X-ray absorption fine-structure spectroscopy study of photostructural changes in amorphous arsenic chalcogenides. Phil. Mag. B 54, 483–490.

Mao, H.K., Xu, J., Bell, P.M., 1986. Calibration of the ruby pressure gauge to 800 kbar under quasi-hydrostatic conditions. J. Geophys. Res. 91, 4673–4676.

Naumov, P., Makreski, P., Jovanovski, G., 2007. Direct atomic scale observation of linkage isomerization of As_4S_4 clusters during the photoinduced transition of realgar to pararealgar. Inorg. Chem. 46, 10624–10631.

Naumov, P.G., ElGhazali, M.A., Mirhosseini, H., Süß, V., Morosan, E., Felser, C., Medvedev, S.A., 2018. Pressure-induced metallization in layered $ReSe_2$. J. Phys. Condens. Matter 30, 035401.

Nayak, A.P., Bhattacharyya, S., Zhu, J., Liu, J., Wu, X., Pandey, T., Jin, C., Singh, A.K., Akinwande, D., Lin, J.F., 2014. Pressure-induced semiconducting to metallic transition in multilayered molybdenum disulphide. Nat. Commun. 5, 3731.

Noll, P.D., Newsom, H.E., Leeman, W.P., Ryan, J.G., 1996. The role of hydrothermal fluids in the production of subduction zone magmas: evidenve from siderophile and chalcophile trace elements and boron. Geochem. Cosmochim. Acta 60, 587–611.

Skettrup, T., 1978. Urbach rule derived from thermal fluctuations in band-gap energy. Phys. Rev. B 18, 2622–2631.

Street, G.B., Gill, W.D., 1966. Photoconductivity and drift mobilities in single crystal realgar As_4S_4. Phys. Status Solidi 18, 601.

Tuktabiev, M.A., Popova, S.V., Brazhkin, V.V., Lyapin, A.G., Katayama, Y., 2009. Compressibility and polymorphism of α-As_4S_4 realgar under high pressure. J. Phys. Condens. Matter 21, 385401.

Wang, J.L., Zhang, S.J., Liu, Y., Jin, C.Q., Li, N.N., Zhang, L.J., Liu, Q.J., Shen, R., He, Z., Liu, X.R., 2017. Pressure-induced metallization in Mg_2Si. J. Phys. Appl. Phys. 50, 235304.

Wang, P., Wang, Y., Qu, J., Zhu, Q., Yang, W., Zhu, J., Wang, L., Zhang, W., He, D., Zhao, Y., 2018. Pressure-induced structural and electronic transitions, metallization, and enhanced visible-light responsiveness in layered rhenium disulphide. Phys. Rev. B 97, 235202.

Wang, Z., Xia, Y., Song, X., You, B., Zheng, X., Wang, X., 2012. Isotopes and REE characteristic and ore-forming materials source of the Taipingdong-Zimudang gold deposit. Acta Mineral. Sin. 32, 93–100 (in Chinese with English abstract).

Yang, L., Dai, L., Li, H., Hu, H., Liu, K., Pu, C., Hong, M., Liu, P., 2019. Pressure-induced metallization in $MoSe_2$ under different pressure conditions. RSC Adv. 9, 5794–5803.

Zhang, Y., Xia, Y., Wang, Z., Yan, B., Fu, Z., Chen, M., 2010. REE and stable isotope geochemical characteristics of Bojitian gold deposit, Guizhou Province. Earth Sci. Front. 17, 385–395 (in Chinese with English abstract).

Zhao, Z., Zhang, H., Yuan, H., Wang, S., Lin, Y., Zeng, Q., Xu, G., Liu, Z., Solanki, G.K., Patel, K.D., Cui, Y., Hwang, H.Y., Mao, W.L., 2015. Pressure induced metallization with absence of structural transition in layered molybdenum diselenide. Nat. Commun. 6, 7312.

Zhuang, Y., Dai, L., Wu, L., Li, H., Hu, H., Liu, K., Yang, L., Pu, C., 2017. Pressure-induced permanent metallization with reversible structural transition in molybdenum disulfide. Appl. Phys. Lett. 110, 122103.